World Wide Journal of Multidisciplinary Research and Development

WWJMRD 2020; 6(7): 43-51
www.wwjmrd.com
International Journal
Peer Reviewed Journal
Refereed Journal
Indexed Journal
Impact Factor MJIF: 4.25
E-ISSN: 2454-6615

Identification of Hydrogeochemical Processes in Part of the Middle Benue Trough, North Central Nigeria.

Rhoda Bernard Gusikit, Ahmed Isah Haruna, Hyeladi Usman Dibal, Janet Agati Yakubu, Victor Bulus Diyelmak

Rhoda Bernard Gusikit
Department of Geology, Faculty of Natural Sciences, P.M.B. 2084, University of Jos, Nigeria.

Ahmed Isah Haruna
Department of Applied Geology, School of Sciences, PO Box 0248, Abubakar Tafawa Balewa University Bauchi, (ATBU), Bauchi, Nigeria.

Hyeladi Usman Dibal
Department of Geology, Faculty of Natural Sciences, P.M.B. 2084, University of Jos, Nigeria.

Janet Agati Yakubu
Department of Geology, Faculty of Natural Sciences, P.M.B. 2084, University of Jos, Nigeria.

Victor Bulus Diyelmak
Department of Geology, Faculty of Natural Sciences, P.M.B. 2084, University of Jos, Nigeria.

Correspondence:
Rhoda Bernard Gusikit
Department of Geology, Faculty of Natural Sciences, P.M.B. 2084, University of Jos, Nigeria.

Abstract
Hydrogeochemical investigations were carried out with an objective to identify the processes affecting the chemistry of groundwater in part of the Middle Benue Trough. Fifty-three groundwater samples were collected from wells, boreholes and springs for chemical analysis. Groundwater types identified from Chadha's plot are four hydrochemical facies: Na-Cl, Ca-Mg-Cl, Na-HCO_3, and Ca-Mg-HCO_3. Processes result in the distribution of elements in groundwater are about 90% natural using Gibbs plots. Gibbs diagrams identified rock–water interaction as an important geochemical process in the study area. Evaporation, ion exchange, silicate weathering and dissolution of carbonate minerals were identified as other important hydrogeochemical processes from the Chadha's plot and Gibbs diagrams which influence the groundwater chemistry of the study area.

Keywords: Groundwater, major ions, hydrogeochemical processes, Middle Benue

Introduction:

In natural hydrological cycling, the groundwater interacts with the surrounding rocks causing a variety of hydrogeochemical processes that alter groundwater chemical components on local or regional scale. The hydrogeochemical processes that are responsible for altering the chemical composition of groundwater vary with respect to space and time [1].The chemistry of groundwater is an index of its complex history, providing important clues to geological environment, indication of groundwater recharge, discharge, movement and storage [2]. The chief function of the Chadha's diagram is to identify the facies of groundwater; it also can help us to understand several geochemical processes along the flow path of groundwater. This diagram is also used to classify the water types [3,4], which are generally distinct zones that cation and anion concentrations are described within the defined composition categories.

Hydrochemical facies can provide insight into the aquifer connectivity and the chemical processes controlling the groundwater chemistry. The mapping of hydrochemical facies shows that at shallow depths within the Coastal Plain (less than about 200 ft) the Ca-Mg cation facies generally predominates. The HCO_3^- anion facies occurs within more of the shallow Coastal Plain sediments than does the SO_4^{2+} or the Cl^- facies. In deeper formations, the NaCl character predominates [5]. The occurrence of the various facies within one formation or within a group of formations of uniform mineralogy indicates that the groundwater flow through the aquifer system modifies the distribution of the facies.

Major ion chemistry of groundwater has been widely used in order to study the subsurface hydrogeochemical processes. [6] Used the major ions to identify the salinization processes in some arid regions of Namibia. [7] Addressed the hydrogeochemical processes in the arid regions of Europe by developing a series of relationships between major and minor ions. [8] Studied the groundwater quality degradation of central Iran using major ions. Geochemical signatures of groundwater are effective tools in identifying the normal hydrogeochemical processes such as $CaCO_3$ dissolution, ion-exchange processes and silicate weathering [9]. [10] analyzed the major ions of the Palar river basin in order to define the relation between water level fluctuations and hydrochemistry. They identified that the important processes controlling the hydrochemistry were the dissolution of minerals and other anthropogenic activities. [11] Employed multivariate statistics to identify the processes controlling the major ions to identify the hydrogeochemical processes controlling the groundwater chemistry in Coimbatore district, India.

Geology of the Study Area

The study area is defined by longitudes 9°0'0" - 9°20'0"E and latitudes 8°0'0" - 8°30'0"N and is part of the Middle Benue Trough. From detail field mapping of the study area, five formations were encountered in the study area with volcanic intrusion resulting in the formation of basaltic rock. The five formations include: Asu River Group which is the oldest formation in the study area and it was encountered both in the northeastern and southeastern as while as in the southwestern part of the study area. Awe-Keana formations are embedded together in the study area. The Awe formation overlaid the Asu River Group. The Awe- Keana formations were found in the northeastern, northwestern and southeastern parts of the study area. Ezeaku formation overlaid the Keana formation in the geology of the Middle Benue Trough. This formation was encountered in northwestern and southeastern parts of the study but only in small portion of the southeastern parts of the study area. Agwu Formation is young formation found in part of the study area and it was encountered in northwestern and southeastern parts of the study area. These five sedimentary formations in the study area were intruded by basalt rocks which are scattered in the northwest, southwest and southwestern parts of the study area.

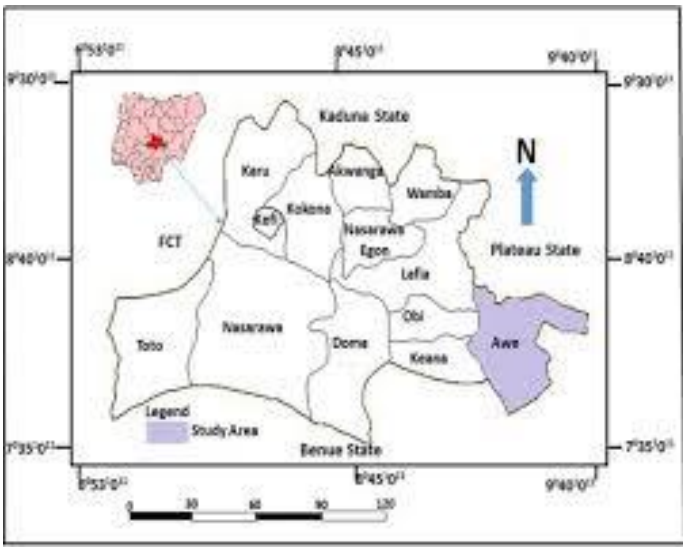

Fig. 1: Location Map of the Study Area

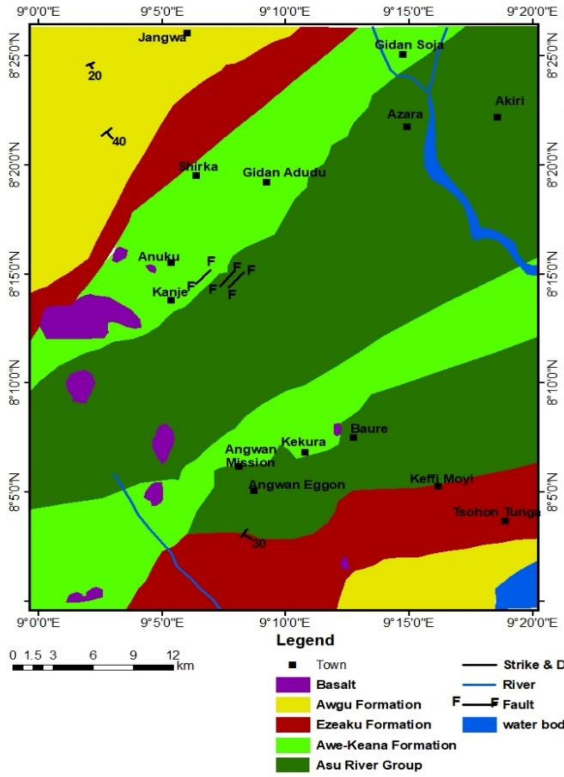

Fig. 2: Geologic map of the study area showing rock types

Materials and Methods

Fifty-three (53) groundwater samples (seventeen (17) from wells, five (5) from springs and thirty one (31) from boreholes) were sampled using 250ml plastic bottles which were previously soaked in acidified water, washed and rinsed with distilled water. At every sampling point, the sample containers were further rinsed with the sampled water before sampling. Two samples were collected at every sampling point, one is acidified with two (2) drops of concentrated hydrochloric acid for homogenization and prevention of absorption/adsorption of elements to the walls of the plastic container while the second sample is not acidify. At each sampling point, the sample containers were rinsed with the sampled water three times before sampling. At every sampling point, coordinate readings were taken using the Global Positioning System (GPS) instrument. The water electrical conductivity (EC µS/cm), Total Dissolved Solids (TDS mg/l) and pH were directly measured using a portable meter in the field, also alkalinity (HCO_3^-mg/l) was also measured in the field using titration method. The acidified water samples were transferred into 60mls plastic bottles and sent to ACME-Laboratories in Canada where Inductive Coupled Plasma Mass Spectrophotometer (ICPMS) was used for major cations analysis. For the non-acidified water sampled, titration method was used for HCO_3 (in the field), SO_4 and Cl^- in the laboratory of Geology Department, University of Jos.

Results and Discussion

Table 1: Physico-chemical parameters of the groundwater in the study area.

S/No	Sources	Longitude	Latitude	pH	TDS (mg/l)	EC (µS/cm)	HCO_3^-	SO_4^{2-}	Cl^-	Ca^{2+}	K^+	Mg^{2+}	Na^+
1.	Well	9°14' 4 9.5"	8°21'49.6"	6.97	582	1164	92.92	37.50	100	25.71	12.7	41.35	137.82
2.	Well	9°14'4 5.6"	8°21'45.3"	6.81	553	1106	50	42	95	17.89	11.04	24.24	214.85
3.	Well	9°12' 27.6"	8°21' 3.7"	6.69	503	1011	52.52	50.00	70	49.46	27.48	32.40	56.82
4.	Well	9°12' 27.2"	8°21' 2.8"	6.69	394	770	72.72	45.00	70	37.65	27.13	32.74	57.17

5.	Well	9°8’34.3”	8°6’5”	6.96	226	465	60.60	66.25	50	28.81	12.02	3.91	69.65
6.	Well	9°8’30.4”	8°6’7.5”	7.27	523	1044	64.64	95.00	50	88.92	5.3	41.96	87.15
7.	Well	9°8’38.8”	8°5’3.5”	7.28	360	730	62.00	80.50	35	48.14	2.71	31.44	69.14
8.	Well	9°8’11.2”	8°6’10.6”	5.9	124	249	62.41	81.00	30	29.23	12.40	4.1	29.41
9.	Well	9°19’25.5”	7°59’55.5”	7.77	1082	2211	72.72	75.00	240	7	67.76	26.79	239.72
10.	Well	9°18’54.5”	8°3′42.9”	7.72	678	1332	40.4	55.00	160	142.38	3.27	40.87	83.22
11.	Well	9°16’49.6”	8°6’17.6”	6.5	285	567	32.32	23.50	40	41.65	3.70	15.39	77.52
12.	Well	9°16’0.3″	8°5’20.9″	7.09	265	518	49.00	12.00	15	34.91	12.68	7.96	74.17
13.	Well	9°12’49.5″	8°7’31.7″	5.35	37	76	10.00	17.00	20	4.28	1.41	1.45	8.06
14.	Well	9°10’42.1″	8°6’49.5″	5.16	12	24	24.24	16.00	5	3.06	0.48	0.54	2.73
15.	Well	9°5’24.3″	8°15’30″	6.36	92	184	48.60	24.50	15	23.12	2.87	2.36	16.61
16.	Well	9°5’24.8″	8°13’49.5″	7.10	710	1414	96.96	16.00	220	30.67	5.61	44.70	214.74
17.	Well	9°5’59.9″	8°26’04.0″	6.15	93	186	8.08	11.50	30	15.33	10.36	2.92	27.44
18.	Spring	9°20′7.0”	8°22′52.0”	6.24	>10000	20000	80.80	10.50	3100	40.2	90.00	22.00	2813
19.	Spring	9°10’30.1″	8°6’51.5″	5.05	10	21	24.00	16.00	10	2.27	0.91	0.58	1.13
20.	Spring	9°8’8.3″	8°5’3.8″	6.54	>10000	20000	113.00	14.00	4600	76	82	33	3770
21.	Spring	9°5’18.7″	8°15’21.1″	5.56	17	36	50.00	29.50	15	5.68	1.59	1.26	13.47
22.	Spring	9°14’41.6″	8°25’05.4″	6.78	19	38	8.08	85.00	15	2.76	1.34	0.62	16.57
23.	Borehole	9°6′22.9”	8°19’27.8	6.68	237	475	68.68	75.00	5	41.39	5.39	20.47	51.27
24.	Borehole	9°6′21.7”	8°19’37.8	6.32	183	364	66.98	72.50	5	35.73	3.10	23.17	44.39
25.	Borehole	9°6′21.4”	8°19’42.6”	6.74	222	447	67.43	74.00	5	16.93	3.08	23.85	47.19
26.	Borehole	9°9′15.4”	8°19′15.7”	6.58	365	729	101.11	17	10	8.81	3.63	35.18	79.74
27.	Borehole	9°10′44.2”	8°18′24.5”	6.42	355	710	105.04	19.00	10	11.95	7.76	68.30	71.79
28.	Borehole	9°10′46”	8°18′25.9”	6.76	367	737	101.00	20.00	10	3.83	7.07	58.69	64.26
29.	Borehole	9°12′00.6”	8°19′18.8”	7.2	302	606	100	15	10	6.82	6.65	54.41	57.21
30.	Borehole	9°19′45.7”	8°23′4.4”	6.13	105	223	48.48	12.50	25	8.96	5.38	7.61	36.42
31.	Borehole	9°18′35.4”	8°22′15.2”	6.82	429	858	68.67	18.00	160	17.86	11.53	28.6	228.55
32.	Borehole	9°14′ 55.8″	8°21′45.1”	6.32	633	1266	88.81	60.00	80	37.63	4.84	48.91	120.27
33.	Borehole	9°14’ 54.4”	8°21’43.6”	6.47	540	1077	80.93	72.10	95	77.76	21.92	29.34	79.45
34.	Borehole	9°14’ 58.3”	8°21’48.9”	6.87	1723	3420	52.63	24	1000	13.94	25.22	12.73	842.39
35.	Borehole	9°14’57.6”	8°21’37.9”	6.6	287	573	8.08	50.00	55	13.36	8.68	32.61	98.94
36.	Borehole	9°9’46.9”	8°21’ 41.9”	7	210	422	56.43	37.50	15	42.84	4.48	28.90	35.31
37.	Borehole	9°19’23.4”	8°0’0.1”	7.04	829	1665	80.87	75.00	180	215.74	11.08	28.14	70.83
38.	Borehole	9°18’54.5”	8°3′42.9”	7.29	329	670	56.55	27.50	45	45.68	6.27	11.17	111.14
39.	Borehole	9°16’49.6”	8°6′17.6”	7.07	270	542	31.67	23.50	10	26.08	2.17	11.98	69.68
40.	Borehole	9°16’8.3”	8°5′21.7”	6.6	212	426	48.48	11.50	50	54.36	2.48	12.83	41.98
41.	Borehole	9°12’21.2″	8°7’27.9″	5.2	12	24	8.08	17.00	10	2.00	1.79	0.47	1.81
42	Borehole	9°10’49.7″	8°6’48.6″	5.7	10	20	24.48	16.00	10	3.06	0.83	0.64	1.13
43	Borehole	9°7’46.1″	8°6’2.2″	6.28	>10000	20000	113.12	14.00	4600	58.20	75	32.00	3460
44	Borehole	9°2’47.6″	8°11’23.12″	6.83	412	826	65.88	16.00	140	43.04	5.58	36.39	100.5
45	Borehole	9°2’49.1″	8°11’26.1″	6.7	1851	3077	38.33	20.00	920	86.05	16.46	82.88	19.35
46	Borehole	9°5’24.8″	8°13’49.5″	6.83	1053	2110	100	16.00	400	53.75	8.12	56.15	300.82
47	Borehole	9°6’9″	8°11’22.1″	6.95	288	581	64.64	33.00	20	52.55	0.67	26.49	10.97
48	Borehole	9°7’18.8″	8°9’2.7″	7.06	310	624	80.81	15.00	15	12.08	1.65	5.58	128.44
49	Borehole	9°8’33.8″	8°6’49.9″	7.24	510	1018	50.37	32.00	35	41.11	4.02	49.82	93.50
50	Borehole	9°8’45.7″	8°6’27.3″	7.06	310	624	73.24	24.00	15	12.97	9.47	5.54	26.34
51	Borehole	9°7’39.1″	8°15’34.3″	7.50	289	576	68.68	15.00	25	52.41	2.41	38.16	47.30
52	Borehole	9°7’46.5″	8°15’49.4″	7.56	218	550	76.75	12.00	15	50.53	3.10	41.07	53.04
53	Borehole	9°9’37.6″	8°17’35.2″	7.74	205	412	64.65	8.50	10	39.55	2.90	31.09	38.48

Table 2: Descriptive statistic for groundwater of the study area

	Minimum	Maximum	Mean	Std. Deviation	Variance
Temp	23.00	46.00	30.4811	3.61216	13.048
pH	5.05	7.77	6.6781	0.64072	0.411
TDS	10.00	10000.00	936.4340	2271.41440	5159323.366
EC	20.00	20000.00	1864.1132	4537.80078	20591635.910
HCO3	8.08	113.12	61.0732	28.04284	786.401
SO4	8.50	95.00	34.8179	25.15480	632.764
Cl	5.00	4600.00	320.1887	968.53873	938067.271
Ca	2.00	215.74	39.3143	39.80228	1584.221
K	0.48	90.00	12.5942	20.27325	411.005
Mg	0.47	82.88	25.5802	19.49876	380.202
Na	1.13	3770.00	273.8279	776.02331	602212.177

Table 3: Calculated values of {HCO_3 (Cl+SO4)} and {(Ca+Mg)-(Na+K)} for Chadha’s plot in groundwater water.

S/No	Sources	HCO/61	SO4/48	Cl/35	Ca/20	K/39	Mg/12	Na/23	{HCO3(Cl+SO4)}	{(Ca+Mg)-(Na+K)}
1	Well	1.523279	0.78125	2.857143	1.28550	0.325641	3.445833	5.992174	2.84249442	-3.98637185

2	Well	0.819672	0.87500	2.714286	0.89450	0.283077	2.02000	9.341304	3.140625	-8.188575226
3	Well	0.860984	1.041667	2.00000	2.47300	0.704615	2.70000	2.470435	3.168402778	-0.629736224
4	Well	1.192131	0.93750	2.00000	1.88250	0.695641	2.728333	2.485652	2.75390625	-0.911451149
5	Well	0.993443	1.380208	1.428571	1.44050	0.308205	0.325833	3.028261	3.876701234	-2.469466298
6	Well	1.059672	1.979167	1.428571	4.44600	0.135897	3.496667	3.78913	6.744481647	-0.01922236
7	Well	1.016393	1.677083	1.00000	2.40700	0.069487	2.62000	3.006087	4.48969184	-0.60211118
8	Well	1.023115	1.68750	0.857143	1.46150	0.317949	0.341667	1.278696	4.294084821	-0.711533231
9	Well	1.192131	1.56250	6.857143	7.42850	1.737436	2.23250	10.42261	13.15569196	-7.416380687
10	Well	0.662295	1.145833	4.571429	7.11900	0.083846	3.405833	3.618261	6.551029266	1.469145866
11	Well	0.529836	0.489583	1.142857	2.08250	0.094872	1.28250	3.370435	0.79921565	-1.8112702
12	Well	0.803279	0.25000	0.428571	1.74550	0.325128	0.663333	3.224783	0.169642857	-2.36676893
13	Well	0.163934	0.354167	0.571429	0.21400	0.036154	0.120833	0.350435	0.32781498	-0.222028161
14	Well	0.397377	0.333333	0.142857	0.15300	0.012308	0.04500	0.118696	0.158730159	-0.033785694
15	Well	0.796721	0.510417	0.428571	1.15600	0.07359	0.196667	0.722174	0.479275174	-0.131997628
16	Well	1.589508	0.333333	6.285714	1.53350	0.143846	3.72500	9.336522	2.206349206	-6.889524455
17	Well	0.132459	0.239583	0.857143	0.76650	0.265641	0.243333	1.193043	0.262757316	-0.962809321
18	Spring	1.32459	0.21875	88.57143	2.01000	2.307692	1.833333	122.30430	19.42285156	-122.7215825
19	Spring	0.393443	0.333333	0.285714	0.11350	0.023333	0.048333	0.049130	0.206349206	0.007036889
20	Spring	1.852459	0.291667	131.4286	3.80000	2.102564	2.75000	163.913	38.41840278	-162.7951172
21	Spring	0.819672	0.614583	0.428571	0.28400	0.040769	0.10500	0.585652	0.641105531	-0.435364533
22	Spring	0.132459	1.770833	0.428571	0.13800	0.034359	0.051667	0.720435	3.894779266	-0.661637544
23	Borehole	1.125902	1.5625	0.142857	2.06950	0.138205	1.705833	2.22913	2.664620536	-0.510661242
24	Borehole	1.098033	1.510417	0.142857	1.78650	0.079487	1.930833	1.93000	2.497132316	-0.180450096
25	Borehole	1.10541	1.541667	0.142857	0.84650	0.078974	1.98750	2.051739	2.596974206	-0.734482937
26	Borehole	1.657541	0.354167	0.285714	0.44050	0.093077	2.931667	3.466957	0.226624504	-1.896663274
27	Borehole	1.721967	0.395833	0.285714	0.59750	0.198974	5.691667	3.121304	0.269779266	-0.217265176
28	Borehole	1.655738	0.416667	0.285714	0.19150	0.181282	4.890833	2.793913	0.29265873	-0.466593066
29	Borehole	1.639344	0.31250	0.285714	0.34100	0.170513	4.534167	2.487391	0.186941964	-0.252113236
30	Borehole	0.794754	0.260417	0.714286	0.44800	0.137949	0.634167	1.583478	0.253828745	-1.188714836
31	Borehole	1.125738	0.37500	4.571429	0.89300	0.295641	2.383333	9.936957	1.854910714	-8.618139839
32	Borehole	1.455902	0.00000	2.285714	1.88150	0.124103	4.075833	5.22913	0.00000	-2.418585938
33	Borehole	1.326721	1.502083	2.714286	3.88800	0.562051	2.44500	3.454348	6.333337674	-0.903357734
34	Borehole	0.862787	0.50000	28.57143	0.697000	0.646667	1.060833	36.62565	14.53571429	-36.40689163
35	Borehole	0.132459	1.041667	1.571429	0.668000	0.222564	2.717500	4.301739	109.375000	-2.855153014
36	Borehole	0.925082	0.781250	0.428571	2.142000	0.114872	2.408333	1.535217	41.015625	0.588966564
37	Borehole	1.325738	1.562500	5.142857	10.78700	0.284103	2.345000	3.079565	398.4375	3.08186378
38	Borehole	0.927049	0.572917	1.285714	2.284000	0.160769	0.930833	4.832174	41.53645833	-3.413759082
39	Borehole	0.51918	0.489583	0.285714	1.304000	0.055641	0.998333	3.029565	16.40104167	-1.953087862
40	Borehole	0.794754	0.239583	1.428571	2.718000	0.06359	1.069167	1.825217	14.734375	-0.028579271
41	Borehole	0.132459	0.354167	0.285714	0.10000	0.045897	0.039167	0.078696	9.5625	-0.056235895
42	Borehole	0.401311	0.333333	0.285714	0.153000	0.021282	0.053333	0.04913	8.666666667	0.030919544
43	Borehole	1.854426	0.291667	131.4286	2.910000	1.923077	2.666667	150.4348	1345.750000	-149.6147874
44	Borehole	1.08000	0.333333	4.000000	2.152000	0.143077	3.032500	4.369565	52.000000	-1.960517386
45	Borehole	0.628361	0.416667	26.285710	4.302500	0.422051	6.906667	0.841304	391.6666667	4.25571094
46	Borehole	1.639344	0.333333	11.428570	2.687500	0.208205	4.679167	13.07913	138.6666667	-9.659709369
47	Borehole	1.059672	0.687500	0.571429	2.627500	0.017179	2.207500	0.476957	36.437500	1.883753385
48	Borehole	1.324754	0.312500	0.428571	0.604000	0.042308	0.465000	5.584348	9.375000	-5.100994697
49	Borehole	0.825738	0.666667	1.000000	2.055500	0.103077	4.151667	4.065217	44.66666667	-1.11091228
50	Borehole	1.200656	0.500000	0.428571	0.648500	0.242821	0.461667	1.145217	19.500000	-0.842209109
51	Borehole	1.125902	0.312500	0.714286	2.620500	0.061795	3.180000	2.056522	12.500000	0.736289528
52	Borehole	1.258197	0.250000	0.428571	2.526500	0.079487	3.422500	2.306087	6.750000	0.542682022
53	Borehole	1.059836	0.177083	0.285714	1.977500	0.074359	2.590833	1.673043	3.276041667	0.501120959

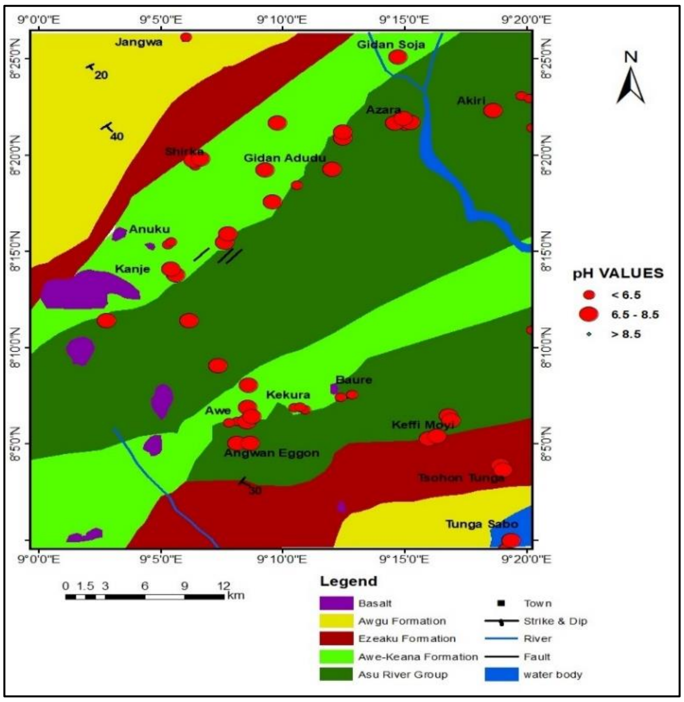

Fig. 3: Bubble map showing distribution of pH in groundwater of the study area

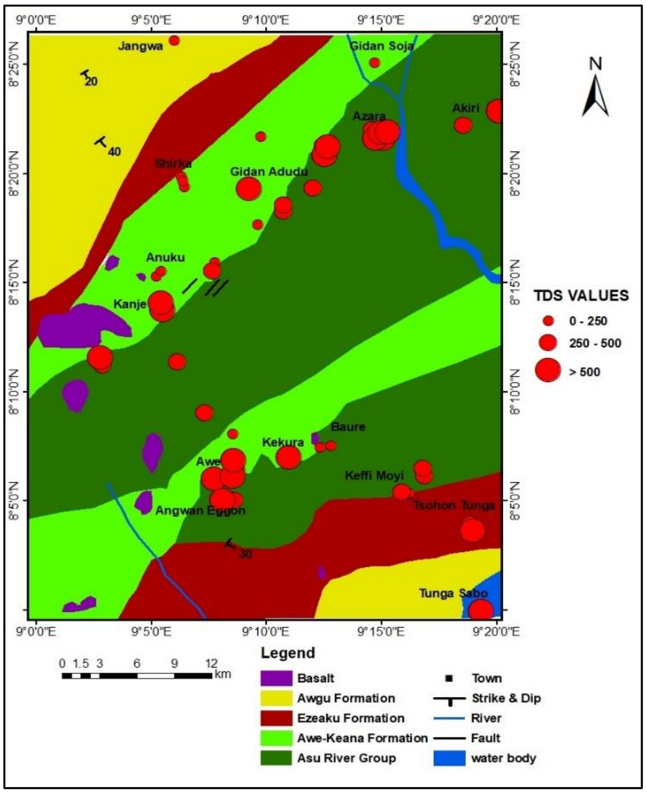

Fig. 4: Bubble map showing distribution of TDS in groundwater of the study area

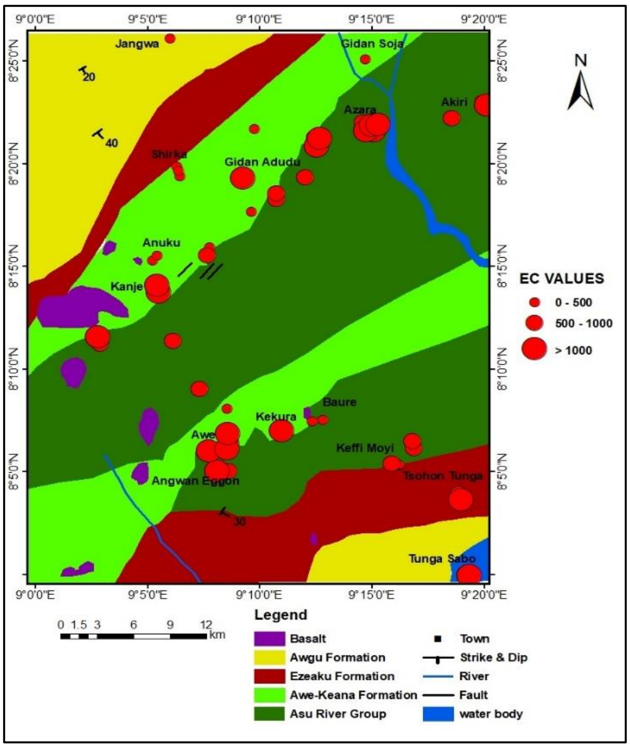

Fig. 5: Bubble map showing distribution of Ec in groundwater of the study area

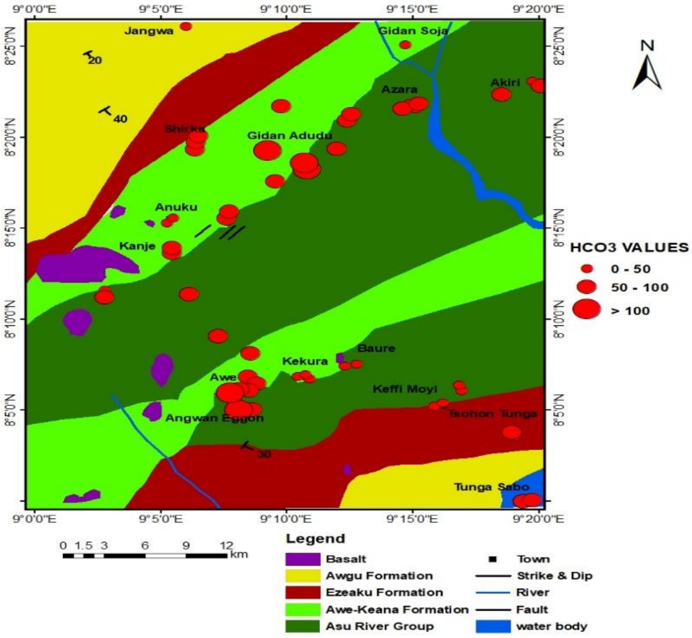

Fig 6: Bubble map showing distribution of HCO_3 in groundwater of the study area

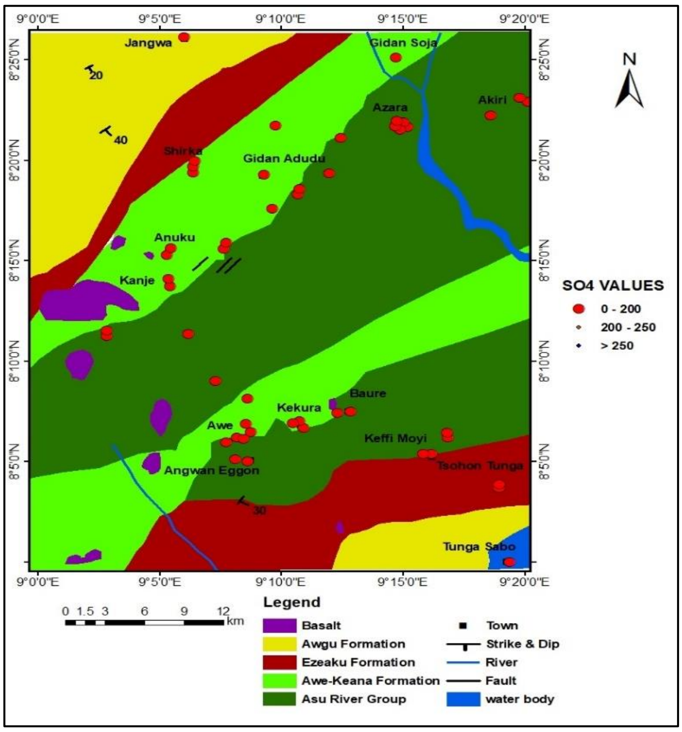

Fig. 7: Bubble map showing distribution of SO_4 in groundwater of the study area

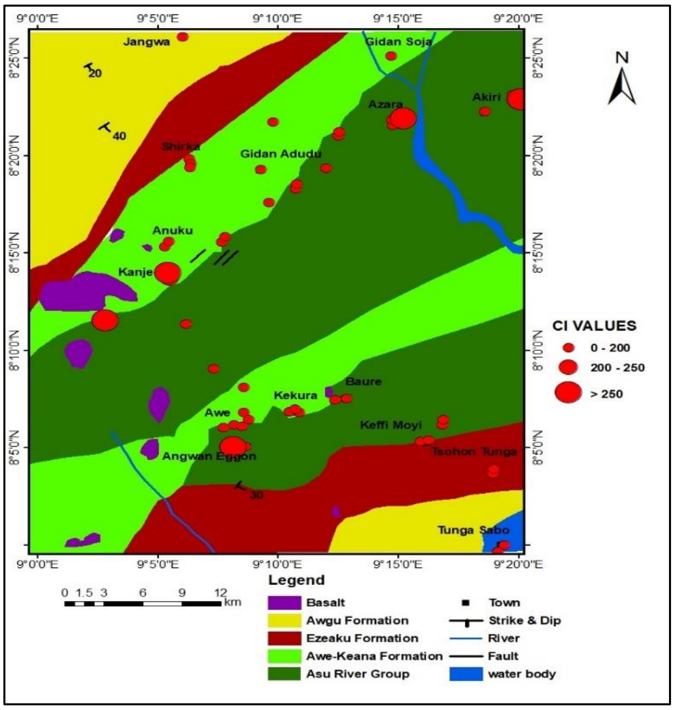

Fig. 8: Bubble map showing distribution of Cl in groundwater of the study area

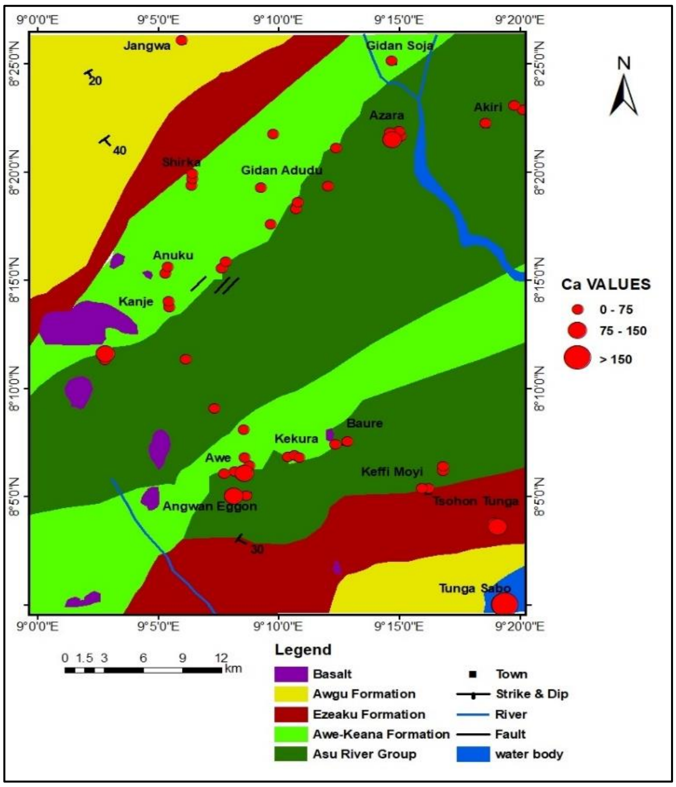

Fig 9: Bubble map showing distribution of Ca in groundwater of the study area

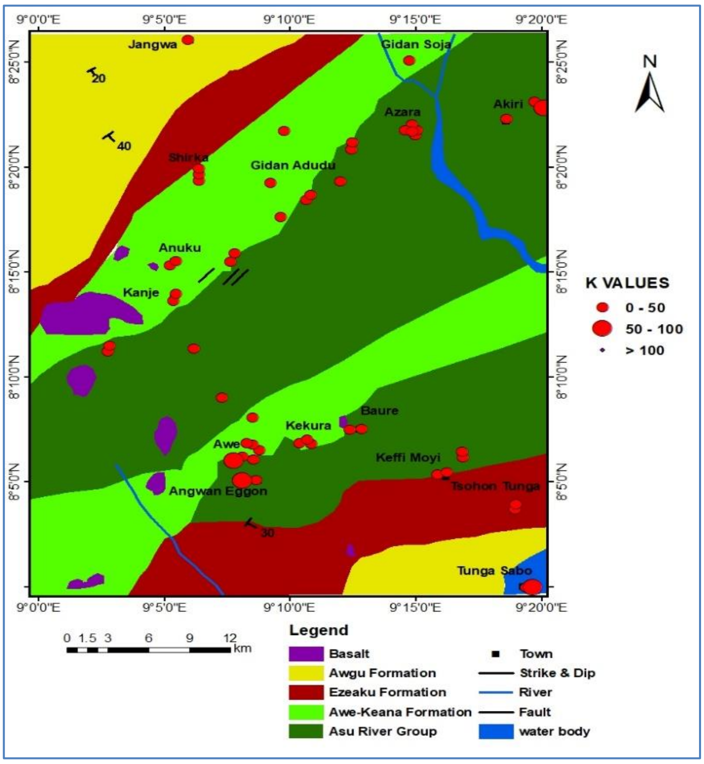

Fig. 10: Bubble map showing distribution of K in groundwater of the study area

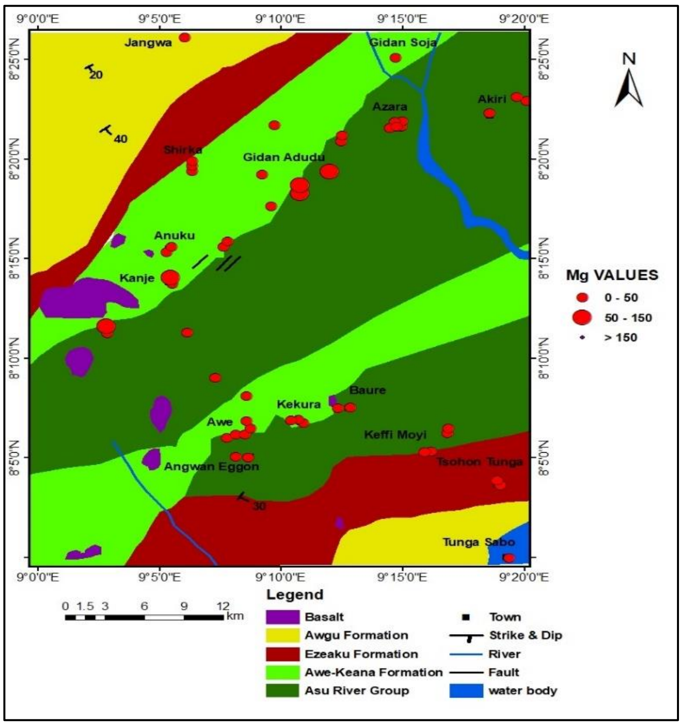

Fig. 11: Bubble map showing distribution of Mg in groundwater of the study area

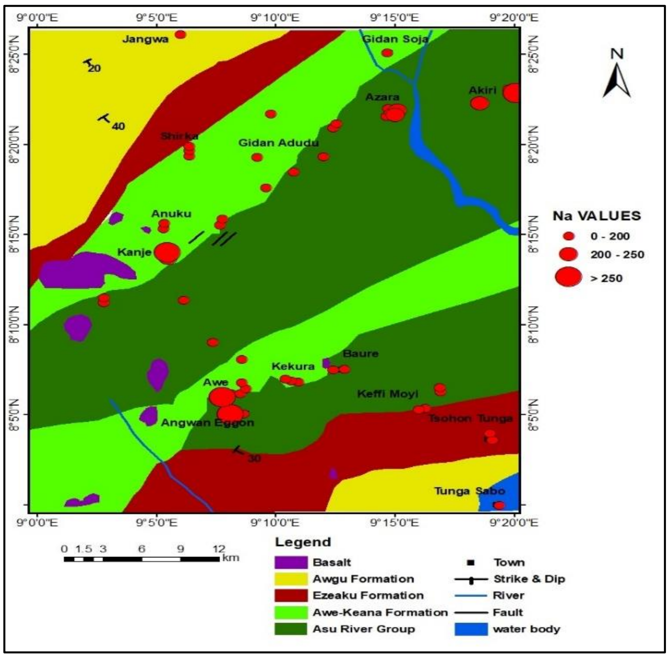

Fig. 12: Bubble map showing distribution of Na in groundwater of the study area

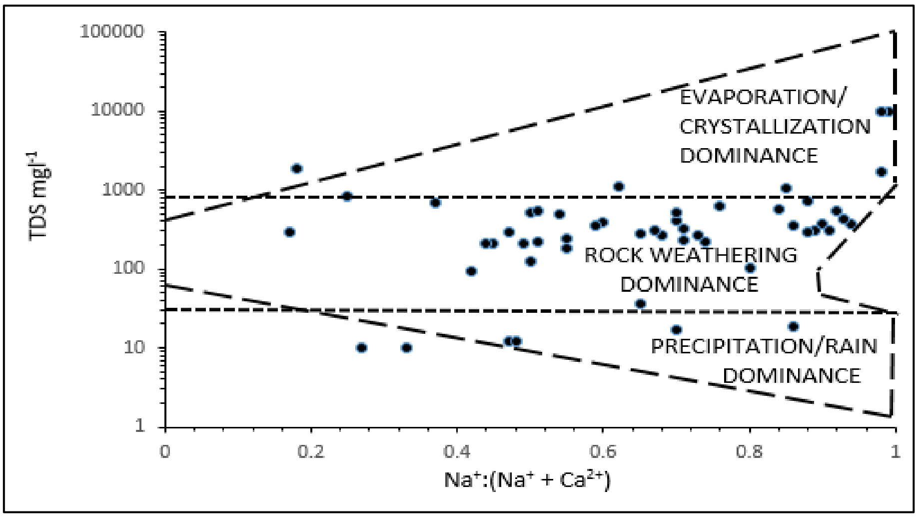

Fig. 13: Gibbs plot of Na/Na + Ca showing the processes involved in the distribution of major cations in groundwater of the study area

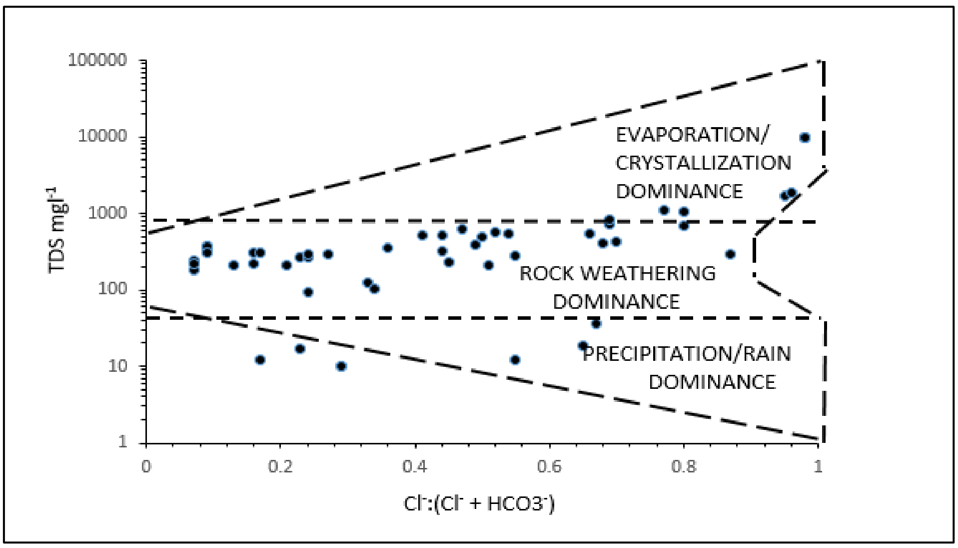

Fig. 14: Gibbs plot of Cl/Cl + HCO_3 showing the processes involved in the distribution of major anions in groundwater of the study **area**

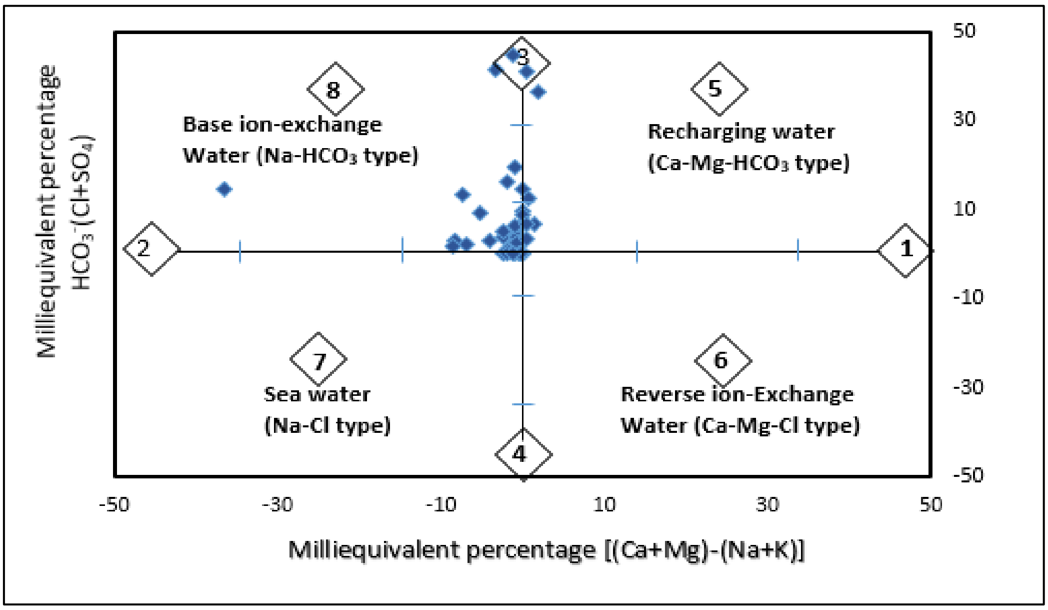

Fig. 15: Groundwater samples from parts of the Middle Benue Trough plotted on modified Piper diagram (Chadha, 1999)

Hydrogeochemistry

Hydrogeochemical parameters of part of the Middle Benue Trough are given in Table 1. The pH of the study area varies from 5.05 to 7.77 with an average of 6.68. The lowest value is from a spring and the highest value from a well. This indicates slightly acidic to slightly alkaline nature of the groundwater. The EC values vary from 20 (borehole) to 20,000 µS/cm (spring and artesian borehole) with an average value of 1864.11 µS/cm, which it is slightly on the high side. Among the 53 groundwater samples considered, seventeen samples show TDS values greater than 1000 (one from well, two from springs and four from boreholes). This implies that the water quality at certain locations is poor. Major cations were analyzed and the dominance of the ions is in the order of Na>Ca>Mg>K. Na is the abundant cation; its values are from 1.13 (spring) to 3770.00 mg/l (spring). Values of Ca vary from 2 (borehole) to 215.74 mg/l (borehole). Magnesium (Mg) has a range of concentration between 0.47 (borehole) to 82.88 mg/l (borehole). Concentration of K is relatively lower and shows a range from 0.48 (well) to 90.00 mg/l (spring). Anions show abundance in the order of $Cl>HCO_3>SO_4$. Chloride (Cl) is the dominant anion in the groundwater, its concentration is between 5.00 (one from well and three from borehole) to 4600.00 mg/l (spring and artesian borehole). Bicarbonate ($HC0_3$), 8.08 (well and borehole) to 113.12 mg/l (spring and artesian borehole) and SO_4, 8.50 (borehole) to 95.00 mg/l (well) are also present. The hydrogeochemical parameters show wide variation, indicating the complex hydrogeochemical processes occurring in the study area.

Distribution of major ions

Great variations in distribution of major ions in groundwater of the study area is given in Table 2. The variation diagram of TDS (Figure 4) shows relatively good quality of groundwater in the northwest part of the study area. Due to high contact time, rock–water interaction may have elevated the level of dissolved ions. The tropical climatic condition is also an important parameter, contributing to the high concentration of TDS. Major geological formations of the study area are Asu River Group and Awe-Keana formations. These formations affect the high concentration of Na and Cl in the groundwater. Moreover, the study area has an ephemeral spring flowing from southwest to southeast. This spring discharges at the southwestern and northeastern boundaries and they are characterized by a high level of dissolved ions. The variation diagram of Na (Figure 12) follows almost the same trend as that of TDS. A study of the variation diagram and the geological map suggests that there is relatively lower concentration of Ca in the Asu River Group and Awe-Keana formations. North-central part of the study area has Mg concentrations in the range of 50–150 mg/l. A comparison of Figure 11 with the geological map shows that the formations have little contribute to the concentrations of Mg in the groundwater. The low level of K compared to Na can be attributed to the high resistance of potassium to weathering, as well as fixation by clay minerals. The Ca more or less follows the same trend as that of K. Variation diagrams of Ca and K are given in Figures 9 and 10. The variation of chloride (Figure 8) is very distinct, as is that of TDS. The origin of Cl is usually the dissolution of halite in the groundwater.

Groundwater types

The groundwater types of the study area are examined using Chadha's plot (Chadha, 1999). Calculated values of {HCO_3(Cl+SO4)} and {(Ca+Mg)-(Na+K)} for Chadha's plot in groundwater water of the study area are given in Table 3. Water types of the study area are quite clear; four distinct hydrogeochemical facies were identified. The Ca-Mg-Cl type of water dominates among the four facies with 71.70% and Na-Cl type is the third prominent with 7.54%. Both of these water types together represent more than 70%. Ca-Mg-HCO_3 water type is the second most prominent with 18.87% and Na-HCO_3 fourth with 1.87% also contribute to the water types. From these results, it is clear that Na and Ca are the dominant cations, and Cl and HCO_3 are the dominant anions. This suggests that dissolution of calcite as well as evaporation processes are prominent in the geo-hydro environment (Figure 15).

Hydrogeochemical processes

The [13] diagram is the most useful tool to identify processes controlling natural water chemistry. A semi logarithmic plot of the total dissolved solids (TDS) versus the weight ratio of cations Na/Na+Ca or weight ratio of the anions Cl/Cl+HCO_3 provides information on the processes controlling the chemistry of water such as atmospheric precipitation, rock dominant and evaporation/crystallization. Gibbs plots have recently been used in a number of groundwater studies of carbonate aquifers to identify hydrochemistry origins [14, 12]. In TDS versus [Na/ (Na + Ca)] plots for groundwater in the study area, most of the samples are plotted in the rock weathering dominance zone. Similar plot was noted for TDS versus [Cl/ (Cl HCO_3)], indicating control of rock-water interaction in hydrogeochemistry of the study area. The Gibbs plots indicated that the hydrochemistry of majority of groundwater samples of the study area are mainly influenced by the rock weathering process. This showed high level of rock-water interaction as the major natural process resulting in the distribution of the groundwater of the study area (Figures13 and 14). Evaporation is a natural process that increases the concentration of ions in the groundwater samples (two springs' water and one artesian borehole) of the study area and is a secondary process. Evaporation also increase the concentration of total dissolved solids in groundwater [15]. When Na and Cl become the major ions in water, the water develops a salty taste. Few samples of groundwater (two well water, two spring and two borehole water) samples in the study fall in the precipitation zone indicating low impact of rain water.

Conclusion

Geochemical analysis of groundwater was carried out in part of the Middle Benue Trough. Major ions were used for Gibbs and Chadha's plots to identify the hydrogeochemical processes controlling the groundwater chemistry. Gibbs plots showed that about 90% of the samples are plotted in the rock weathering dominance zone while the remaining 10% fall in the precipitation and evaporation zones. Four hydrochemical facies (CaMgCl, $CaMgHCO_3$, NaCl, and NaHCO3) were identified using Chadha's plot.

References

1. Phyu PT, Heru H, Wahyu W, Satoru K. Assessment of Groundwater Facies in Wates Coastal Area, Kulon Progo, YOGYAKARTA, Indonesia. Journal of degraded and mining and management, 2018; 5(4): 1389-1401.
2. Afsin, M. Hydrochemical evolution and water quality along the groundwater flow path in the Sandikli plain, Afyon. Turk Env Geol., 1997; 31(3/4): 221–230.
3. Wen X, Wu Y, Su J, Zhang Y, Liu F. Hydrochemical characteristics and salinity of groundwater in the Ejina Basin, Northwestern China. J. *Environ. Geol.* 2005; 48: 665–675.
4. Karmegam U, Chidambaram S, Prasanna MV, Sasidhar P, Manikandan S, Johnsonbabu G, Dheivanayaki V, Paramaguru P, Manivannan R, Srinivasamoorthy K, Anandhan, P. A study on the mixing proportion in groundwater samples by using Piper diagram and Phreeqc model. Chin. J. Geochem., 2011; 30: 490–495.
5. Back W. Hydrogeochemical facies and groundwater flow pattern in the northern part of the Atlantic Coastal Plain: U.S. Geological Survey Professiona, 1966; Paper: 498–A.
6. Shanyengana ES, Seely MK, Sanderson RD. Major-ion chemistry and ground-water salinization in ephemeral floodplains in some arid regions of Namibia. Journal of Arid Environments, 2004; 57: 211–223.
7. Sanchez-Martos F, Bosch AP, Calaforra JM. Hydrogeochemical processes in an arid region of Europe (Almeria, SE Spain). Applied Geochemistry, 1999; 14: 735–745.
8. Baghvand A, Nasrabadi T, Bidhendi GN, Vosoogh A, Karbassi A, Mehrdadi N. Groundwater quality degradation of an aquifer in Iran central desert. Desalination. 2010; 260: 264–275.
9. Lakshmanan E, Kannan R, Senthilkumar M. Major ion chemistry and identification of hydrogeochemical processes of ground water in a part of Kancheepuram district, Tamil Nadu, India. Environmental Geoscience, 2003; 10: 157–166.
10. Rajmohan N, Elango L. Hydrogeochemistry and its relation to groundwater level fluctuation in the Palar and Cheyyar river basins, southern India. Hydrological Processes, 2006; 20: 2415–2427.
11. Cloutier V, Lefebvre R, Therrien R, Savard MM. Multivariate statistical analysis of geochemical data as indicative of the hydrogeochemical evolution of groundwater in a sedimentary rock aquifer system. J Hydrol, 2008; 353: 294–313.
12. Sajil-Kumar PJ, Jamesa EJ. Identification of hydrogeochemical processes in the Coimbatore district, Tamil Nadu, India: Hydrological Sciences Journal, 2016; VOL. 61, NO. 4: 719–731.
13. Gibbs RJ. Mechanisms Controlling World Water Chemistry. *Science*, 1970; Vol. 170, Issue 3962: 1088-1090.
14. Sajil-Kumar PJ. Interpretation of groundwater chemistry using piper and chadha׳s diagrams: a comparative study from perambalur taluk. Elixir Geoscience, 2013; 54: 12208-12211.
15. Subramani T, Rajmohan N, Elango L. Groundwater geochemistry and identification of hydrogeochemical processes in a hard rock region Southern India. Environmental Monitoring and Assessment, 2010; 162: 123–137.